

# **Distinct regulation of cardiac fibroblast proliferation and transdifferentiation by classical and novel protein kinase C isoforms: possible implications for new antifibrotic therapies**

S. Tuuli Karhu, Heikki Ruskoaho, Virpi Talman\*

## *Affiliations*

*STK, HR, and VT: Drug Research Program and Division of Pharmacology and Pharmacotherapy, Faculty of Pharmacy, University of Helsinki, Finland*

*\*Corresponding author*

**Running title:** PKC agonists inhibit cardiac fibroblast activation

**Corresponding author:**

Virpi Talman

Division of Pharmacology and Pharmacotherapy

Faculty of Pharmacy

University of Helsinki

P.O. Box 56 (Viikinkaari 5E)

FI-00014 Helsinki, FINLAND

Tel: +358504480768

Email: [virpi.talman@helsinki.fi](mailto:virpi.talman@helsinki.fi)

Number of text pages: 35

Number of tables: 0

Number of figures: 4

Number of references: 55

Number of words in the Abstract: 249

Number of words in the Introduction: 728

Number of words in the Discussion: 1459

**Abbreviations:**  $\alpha$ -SMA,  $\alpha$ -smooth muscle actin; aPKC, atypical protein kinase C isoform; BrdU, 5-bromo-2'-deoxyuridine; CF, cardiac fibroblast; cPKC, classical protein kinase C isoform; DDR2, discoidin domain receptor 2; ECM, extracellular matrix; ERK, extracellular signal-regulated kinase; HCA, high-content analysis; LDH, lactate dehydrogenase; MTT, 3-(4,5-dimethylthiazol-2-yl)-2,5-diphenyltetrazolium bromide; nPKC, novel protein kinase C isoform; PKC, protein kinase C

## Abstract

Cardiac fibrosis is characterized by accumulation and activation of fibroblasts and excessive production of extracellular matrix, which results in myocardial stiffening and eventually leads to heart failure. While previous work suggests that protein kinase C (PKC) isoforms play a role in cardiac fibrosis and remodeling, the results are conflicting. Moreover, the potential of targeting PKC with pharmacological tools to inhibit pathological fibrosis has not been fully evaluated. Here we investigated the effects of selected PKC agonists and inhibitors on cardiac fibroblast (CF) phenotype, proliferation, and gene expression using primary adult mouse CFs, which spontaneously transdifferentiate into myofibroblasts in culture. A 48-h exposure to the potent PKC activator phorbol 12-myristate 13-acetate (PMA) at 10 nM concentration reduced the intensity of  $\alpha$ -smooth muscle actin staining by 56% and periostin mRNA levels by 60% compared to control. The decreases were inhibited with the pan-PKC inhibitor Gö6983 and the inhibitor of classical PKC isoforms Gö6976, suggesting that classical PKCs regulate CF transdifferentiation. PMA also induced a 33% decrease in BrdU-positive CFs, which was inhibited with Gö6983 but not with Gö6976, indicating that novel PKC isoforms (nPKCs) regulate CF proliferation. Moreover, PMA downregulated the expression of collagen encoding genes *Col1a1* and *Col3a1* nPKC-dependently, showing that PKC activation attenuates matrix synthesis in CFs. The partial PKC agonist isophthalate derivative HMI-1b11 induced parallel changes in phenotype, cell cycle activity, and gene expression. In conclusion, our results reveal distinct PKC-dependent regulation of CF transdifferentiation and proliferation and suggest that PKC agonists exhibit potential as an antifibrotic treatment.

## Significance Statement

Cardiac fibrosis is a pathological process that contributes to the development of heart failure. The molecular mechanisms regulating fibrosis in the heart are however not fully understood, which hinders the development of new therapies. Here, we demonstrate that classical and novel protein kinase C (PKC) isoforms distinctly regulate cardiac fibroblast transdifferentiation and proliferation, the two central processes in fibrosis. Our results indicate that pharmacological PKC activation may be a promising strategy to inhibit myocardial fibrosis.



## Introduction

Cardiac fibrosis is characterized by transdifferentiation of fibroblasts into secretory and contractile myofibroblasts and concomitant accumulation of extracellular matrix (ECM) in the myocardium (Kong et al., 2014). While several cell types can contribute to fibrotic remodeling indirectly by secreting pro-fibrotic factors, resident cardiac fibroblasts (CFs) are the key cell type responsible for fibrosis. Upon pathological stimuli, CFs become activated and transdifferentiate into myofibroblasts, which exhibit characteristics of both fibroblasts and smooth muscle cells and produce high amounts of ECM proteins (Talman and Ruskoaho, 2016). The fibrotic response is a crucial part of the healing process after a myocardial infarction (Shinde and Frangogiannis, 2014; van den Borne et al., 2010). However, prolonged fibroblast activation in remote areas outside the initial insult area or due to other stimuli, e.g. pressure overload, leads to adverse myocardial remodeling and progressive impairment of cardiac function. Cardiac fibrosis has been identified as an independent risk factor in heart failure (Gulati et al., 2013): it was associated independently, beyond left ventricular ejection fraction, with mortality and sudden cardiac death in patients with dilated cardiomyopathy. Slowing or reversing cardiac fibrosis is a therapeutic goal in heart failure therapy (Cohn et al., 2000).

Protein kinase C (PKC) is a group of ten related serine-threonine protein kinases, which are known to participate in various signaling pathways and thus regulate e.g. cell proliferation, differentiation, migration, gene transcription and translation, as well as cell death (Mochly-Rosen et al., 2012). PKC isoforms can be divided into three subgroups based on their regulatory region structure and activator requirements (Steinberg, 2008). The classical isoforms (cPKCs;  $\alpha$ ,  $\beta$ I,  $\beta$ II, and  $\gamma$ ) require both diacylglycerol (DAG) and calcium for their activation, whereas the novel isoforms (nPKCs;  $\delta$ ,  $\epsilon$ ,  $\eta$ , and  $\theta$ ) are activated by DAG alone. A more distant subgroup of atypical isoforms (aPKCs;  $\zeta$  and  $\lambda$  /I) does not respond to either DAG or calcium. The expression of PKC isoenzymes in myocardium varies between species

but also between normal and diseased state (Palaniyandi et al., 2009). In the adult human heart, for instance, all isoforms except for  $\gamma$  and  $\theta$  have been detected (Shin et al., 2000; Simonis et al., 2007). On the other hand, dilated cardiomyopathy leads to upregulation of PKC $\beta$  (Bowling et al., 1999), while aortic stenosis leads to upregulation of several isoforms but not PKC $\beta$  (Simonis et al., 2007).

The roles of individual PKC isoforms have been investigated using genetic knockdown and overexpression models, as well as pharmacological inhibitors. The majority of the reports suggests that PKC promotes fibrosis. The ATP-competitive PKC $\beta$  inhibitor ruboxistaurin reduced cardiac fibrosis and dysfunction after myocardial infarction in rats (Boyle et al., 2005) and in mice subjected to pressure overload (Liu et al., 2009). It also attenuated collagen deposition in a rat diabetic cardiomyopathy model (Connelly et al., 2009). Moreover, selective inhibition of PKC $\beta$ II with a translocation peptide inhibitor suppressed myocardial fibrosis in hypertensive rats (Ferreira et al., 2011). Regarding novel PKC isoforms, pharmacological inhibition of PKC $\epsilon$  with a selective translocation peptide inhibitor reduced fibrosis in hypertensive rats and collagen secretion from cultured primary CFs stimulated with transforming growth factor  $\beta$  (TGF- $\beta$ ) (Inagaki et al., 2008). However, there are also contradictory reports suggesting that PKC may in fact have a role in limiting cardiac fibrosis. PKC $\epsilon$  knockout mice showed increased fibrosis and elevated expression of collagen I and III in response to pressure overload (Klein et al., 2005). Moreover, *in vitro* selective inhibition of PKC $\delta$  with a translocation peptide inhibitor promoted neonatal rat CF proliferation (Braun and Mochly-Rosen, 2003).

The aim of this study was to investigate the effect of pharmacological PKC activation on viability, cell cycle activity, phenotype, and gene expression of adult mouse primary CFs *in vitro*. The compounds include the potent tumour-promoting PKC activator phorbol 12-myristate 13-acetate (PMA) and the isophthalate derivative bis(1-ethylpentyl) 5-(hydroxymethyl)isophthalate (HMI-1b11), both of which activate PKC by binding to the DAG

binding sites within duplicated C1 domains in cPKCs and nPKCs (Boije af Gennäs et al., 2009; Boije af Gennäs et al., 2011). To clarify the role of different PKC subfamilies, two PKC inhibitors Gö6976 and Gö6983, which differ in their selectivity towards cPKCs and nPKCs, were used. Our results demonstrate that cPKCs and nPKCs distinctly regulate proliferation and transdifferentiation of CFs, the two central cellular processes in the development of cardiac fibrosis, and indicate that fibroblast-targeted PKC activation may be a potential therapeutic strategy to inhibit cardiac fibrosis.

## Materials and Methods

### Materials

Cell culture media and supplements were purchased from Gibco (Thermo Fisher Scientific, Paisley, UK). Enzyme P, Red Blood Cell Lysis Solution (10x), gentleMACS™ C tubes, and gentleMACS™ Dissociator were from Miltenyi Biotec (Bergisch Gladbach, Germany). DNase I was purchased from AppliChem (Darmstadt, Germany), Collagenase type 2 from Worthington Biochemical Corporation (Lakewood, New Jersey, USA), and gelatin from Merck Millipore (Darmstadt, Germany). PMA was purchased from Sigma-Aldrich (Steinheim, Germany). Diheptan-3-yl 5-(hydroxymethyl)isophthalate (HMI-1b11) was synthesized at the Division of Pharmaceutical Chemistry and Technology, Faculty of Pharmacy, University of Helsinki as described previously (Boije af Gennäs et al., 2009). PKC inhibitors Gö6976 and Gö6983 were purchased from Merck Millipore (Billerica, MA, USA). All reagents used in the cytotoxicity assays were from Sigma-Aldrich. AlphaLISA® SureFire® Ultra™ p-ERK 1/2 (Thr202/Tyr204) and AlphaLISA® SureFire® Ultra™ Total ERK 1/2 assay kits were from PerkinElmer (Groningen, The Netherlands).

Trans-Blot® Turbo™ Midi PVDF Transfer Packs and 12% Mini-Protean® TGX Stain-Free™ Protein Gels were purchased from Bio-Rad. Pierce™ BCA Protein Assay Kit and SuperSignal™ West Femto Maximum Sensitivity Substrate were from Thermo Scientific. The primary antibodies used in western blotting were: monoclonal rabbit anti-PKC alpha (Abcam #ab32376), monoclonal rabbit anti-PKC delta (Abcam #ab182126), monoclonal rabbit anti-PKC epsilon (Abcam #ab124806), monoclonal rabbit anti-PKC eta (Abcam #ab179524), and polyclonal rabbit anti-β-actin (Cell Signaling Technology #4967). The secondary HRP-linked antibody anti-rabbit IgG (#7074) was from Cell Signaling Technology.

5-Bromo-2'-deoxyuridine (BrdU) was purchased from Abcam (Cambridge, UK). The primary antibodies used in immunofluorescence stainings were: monoclonal mouse anti- $\alpha$ -smooth muscle actin (Sigma-Aldrich #A2547), polyclonal rabbit anti-DDR2 (Santa Cruz Biotechnology #sc-8989), monoclonal rat anti-BrdU (Abcam #ab6326), and polyclonal rabbit anti-Ki67 (Abcam #ab15580). The secondary antibodies used were all purchased from Life Technologies; Alexa Fluor 488 goat anti-mouse IgG (#A11029), Alexa Fluor 546 donkey anti-rabbit IgG (#A10040), and Alexa Fluor 647 goat anti-rat IgG (#A21247), with the exception of Alexa Fluor 594 goat anti-rabbit IgG (#ab150080), which was from Abcam. 4',6-diamidino-2-phenylindole (DAPI) was from Sigma-Aldrich.

NucleoSpin® RNA kit was from Macherey-Nagel (Düren, Germany). Transcriptor First Strand cDNA Synthesis kit and LightCycler® 480 Probes Master kit were from Roche. TaqMan™ gene expression assays for *18S* (Hs99999901\_s1), *Actb* (Mm00607939\_s1), *Acta2* (Mm01546133\_m1), *Col1a1* (Mm00801666\_g1), *Col1a2* (Mm00483888\_m1), *Col3a1* (Mm00802300\_m1), *Fn1* (Mm01256744\_m1), *Mmp2* (Mm00439498\_m1), *Mmp9* (Mm00442991\_m1), *Myh10* (Mm00805131\_m1), *Postn* (Mm01284919\_m1), *Tgfb1* (Mm01178820\_m1), and *Tcf21* (Mm00448961\_m1) were purchased from Thermo Fisher Scientific.

### Primary cardiac fibroblasts

Primary cultures of CFs were prepared from 10–20 weeks old female C57BL/6J OlaHsd mice weighing 20–22 g (Envigo, Horst, The Netherlands). Animals were euthanized by CO<sub>2</sub> narcosis followed by cervical dislocation. Thoracic cavities were opened and hearts were perfused through aortas with 2.5 ml of 500 U/ml collagenase II in phosphate-buffered saline (PBS) using a 27 G 12 mm needle. Ventricles were dissected, cut into small pieces, and transferred into gentleMACS C tubes (2 hearts/tube) containing 5 ml enzyme solution [Dulbecco's modified Eagle's medium (DMEM) containing 400 U/ml collagenase II, 60 U/ml DNase I, and 10  $\mu$ l/ml enzyme P]. The tissue pieces were first incubated at 37°C under 300

rpm shaking conditions for 20 min, followed by mechanical digestion with gentleMACS Dissociator (program *m\_muscle\_01*). Enzymatic digestion was continued with a 30-min incubation at 37°C under 600 rpm shaking conditions followed by a second mechanical digestion. The lysate was quickly centrifuged at 300g, 4°C and tissue debris was separated from the cell suspension with a 250 µm tissue strainer. The cell suspension was centrifuged at 300g, 4°C for 10 min. The cell pellet was resuspended in a buffer solution containing 0.5% bovine serum albumin (BSA) and 2 mM EDTA in PBS, pH 7.2. To remove erythrocytes, red blood cell lysis solution was added according to the manufacturer's protocol and incubated for 2 min at room temperature (r.t.). After centrifuging the sample for 10 min at 300g, 4°C and aspirating the supernatant, the cells were washed with medium used for fibroblast culture [DMEM/F-12 supplemented with 10% foetal bovine serum (FBS), 100 U/ml penicillin, and 100 µg/ml streptomycin], and centrifuged again for 10 min at 300g, 4°C. The cells were then resuspended in culture medium, plated on well plates, and let attach for 2 h in cell culture conditions (37°C, humidified atmosphere of 5% CO<sub>2</sub>). To remove dead cells the medium was changed before letting the cells grow overnight prior to compound treatments. For gene expression and phenotypic studies cells were grown on gelatin-coated microscope cover glasses, whereas for viability and cellular kinase assays and high-content analysis (HCA) they were grown on plastic 96-well plates, and for western blotting on plastic 6-well plates.

### Cell viability assays

The cells were exposed to the compounds (1–100 nM PMA, 1–30 µM HMI-1b11, 0.1–10 µM Gö6976, 0.1–10 µM Gö6983) for 24 h after which necrosis and mitochondrial metabolism were investigated using the lactate dehydrogenase (LDH) and the 3-(4,5-dimethylthiazol-2-yl)-2,5-diphenyltetrazolium bromide (MTT) assays, respectively, as described previously (Talman et al., 2011). For the LDH assay, 50 µl of culture medium was transferred from each well onto a new 96-well plate followed by addition of 50 µl substrate solution containing 1.3 mM β-nicotinamide adenine dinucleotide, 660 µM iodonitrotetrazolium, 54 mM L(+)-lactic acid, 280 µM phenazine methosulphate, and 0.2 M Tris-HCl (pH 8.0). After a 30-min

incubation at r.t. the reaction was stopped by adding 50 µl of 1 M acetic acid to each well and absorbance was measured at 490 nm using Victor2 plate reader (PerkinElmer, Turku, Finland). Spontaneous LDH release was measured from untreated cells, maximal LDH release from cells lysed with 0.9% Triton X-100, and background absorbance from wells without cells (medium only). After subtracting background, cytotoxicity was calculated as follows: cytotoxicity-% = [(sample – spontaneous LDH release) / (maximal LDH release – spontaneous LDH release)] × 100. For the MTT assay, MTT was added to the cells at a final concentration of 0.5 mg/ml followed by a 2-h incubation in cell culture conditions. The medium was aspirated and formazan crystals were solubilized in dimethyl sulfoxide (DMSO). Absorbance was measured at 550 nm and absorbance at 650 nm was subtracted as background.

### **Cellular kinase assay**

The cells were exposed to the compounds (10 nM PMA or 10 µM HMI-1b11 with or without 1 µM Gö6976 or 1 µM Gö6983) for 30 min after which they were lysed and the amount of phosphorylated extracellular signal-regulated kinases 1/2 (p-ERK1/2) and total ERK1/2 were detected using AlphaLISA® SureFire® Ultra™ p-ERK 1/2 (Thr202/Tyr204) and AlphaLISA® SureFire® Ultra™ Total ERK 1/2 assay kits according to the manufacturer's protocol. The cells were lysed in 80 µl lysis buffer and 30 µl of the lysate was transferred from each well to two 96-well 1/2 AreaPlates™ (PerkinElmer) for assays. The lysates were then incubated with the Acceptor bead mix for 1 h at r.t., followed by addition of the Donor bead mix and a further 5-h incubation at r.t. The Alpha signal was measured using EnSpire Alpha plate reader (PerkinElmer, Turku, Finland) with standard AlphaLISA settings.

### **Western blotting**

The cells were exposed to the compounds (10 nM PMA or 10 µM HMI-1b11 with or without 1 µM Gö6983) for 48 h after which they were lysed with 1% sodium dodecyl sulphate (SDS) in 50 mM Tris-HCl (pH 7.5) and genomic DNA was sheared with a 25 G needle. Protein

concentrations were determined with bicinchoninic acid (BCA) protein assay kit. From each sample 10 µg of total protein was resolved on a 12% Mini-protean TGX stain-free gel and transferred by Trans-Blot Turbo transfer system to polyvinylidene difluoride (PVDF) membranes. After blocking the nonspecific background with 5% non-fat milk in Tris-buffered saline with 0.05% Tween 20 (TTBS) for 1 h at r.t., the membranes were incubated with primary antibodies (anti-PKCα 1:1000, anti-PKCδ 1:5000, anti-PKCε 1:1000, anti-PKCη 1:2000, anti-β-actin 1:1000 dilution in 5% milk-TTBS) overnight at 4°C. After washing with TTBS, the membranes were incubated for 1 h at r.t. with HRP-conjugated secondary antibody (1:2000 dilution in 5% milk-TTBS). Bands were detected with an enhanced chemiluminescent (ECL) substrate using ChemiDoc XRS+ (Bio-Rad) or Luminescent Imager Analyzer LAS-3000 (Fujifilm) and relative densities were quantified using Fiji ImageJ 1.52 software. Optical densities of PKC isoform immunoreactive bands were adjusted to corresponding β-actin bands from the same membranes.

### **Non-automated fluorescence microscopy and phenotypic analysis**

The cells were grown in mere cell culture medium for 1–3 days after cell isolation or they were exposed to PKC agonists (10 nM PMA or 10 µM HMI-1b11) and inhibitors (1 µM Gö6976 or 1 µM Gö6983) 24 h after isolation for 48 h. The cells were fixed with 4% paraformaldehyde (PFA) for 15 min at r.t. and permeabilized with 0.1% Triton X-100 for 10 min. The cells were then washed 2 × 10 min with Dulbecco's PBS containing 0.2% BSA (DB) and incubated at r.t. for 60 min with primary antibodies; anti-α-SMA (1:200) and anti-DDR2 (1:50) diluted in DB. After three 5-min washes with DB, the cells were incubated with Alexa Fluor-conjugated secondary antibodies (1:200) and DAPI (1 µg/ml) at r.t. for 45 min. After three 5-min washes, the microscope cover glasses were mounted on microscope slides with Prolong™ Gold Antifade Mountant and imaged with Leica DM6000B fluorescence wide field microscope (Leica Microsystems, Wetzlar, Saksa) and CMOS camera (Hamamatsu Orca-Flash4.0 V2, Hamamatsu Photonics, Hamamatsu, Japan). The objective was 20×/0.7 HC PL APO CS and the software was Leica Application Suite X (Leica Microsystems, Wetzlar,



Germany). The images were analyzed using CellProfiler™ image analysis software. For quantification, the cells were first identified based on DAPI fluorescence, which defined the nuclear area, and the cell area was defined by extending the nuclear area with the area defined by DDR2 staining. Integrated intensity of  $\alpha$ -SMA staining was then quantified from each individual cell.

### **Automated fluorescence microscopy and high content analysis**

For HCA of CF proliferation, the cells were stained, imaged, and analyzed as described previously (Karhu et al., 2018). The cells were exposed to the compounds (10 nM PMA or 10  $\mu$ M HMI-1b11 with or without 1  $\mu$ M Gö6976 or 1  $\mu$ M Gö6983) for 48 h, and 10  $\mu$ M BrdU was added to the culture medium for the last 24 h before fixation. The cells were fixed with 4% PFA for 15 min at r.t. and permeabilized with 0.1% Triton X-100 for 10 min. DNA was hydrolysed with 2 M HCl for 30 min (r.t.) followed by neutralization with 0.1 M sodium borate (pH 8.5) for 30 min. Non-specific binding sites were blocked with 4% FBS in PBS for 45 min (r.t.). The cells were incubated 60 min with primary antibodies; anti- $\alpha$ -SMA (1:200), anti-BrdU (1:250), and anti-Ki67 (1:250) diluted in 4% FBS. After 3  $\times$  5-min washes with PBS, the cells were incubated with Alexa Fluor-conjugated secondary antibodies (1:200) and DAPI (1  $\mu$ g/ml) at r.t. for 45 min. The 96-well plates were imaged and analyzed with CellInsight CX5 High-Content Screening Platform (Thermo Scientific) using a 10 $\times$  objective (Olympus UPlanFL N 10 $\times$ /0.3). For quantification of BrdU-positive and Ki67-positive CFs, the cells were first identified based on DAPI fluorescence, which defined the nuclear area. The thresholds for BrdU+ and Ki67+ cells were set manually in each experiment to adjust for slight variation in staining intensities.

### **Quantitative real-time PCR**

The cells were exposed to the compounds (10 nM PMA or 10  $\mu$ M HMI-1b11 with or without 1  $\mu$ M Gö6976 or 1  $\mu$ M Gö6983) for 48 h after which they were lysed and RNA was isolated using NucleoSpin® RNA kit (Macherey-Nagel, Düren, Germany) according to the

manufacturer's protocol. Samples were lysed in 350  $\mu$ l lysis buffer containing 1%  $\beta$ -mercaptoethanol. Total RNA was transcribed into complementary DNA (cDNA) with Transcriptor First Strand cDNA Synthesis kit (Roche, Mannheim, Germany) following the manufacturer's protocol using random hexamer primers. Quantitative polymerase chain reaction (qPCR) was performed using TaqMan™ assays (Thermo Fisher Scientific), LightCycler® 480 Probes Master kit (Roche), and LightCycler® 480 Real-Time PCR machine (Roche). The results were analyzed using the  $\Delta\Delta$ Ct method and adjusted to the average of two housekeeping genes (*18S* and *Actb*) from the same samples.

## Ethics

The animals were housed and terminated in accordance with the 3R principles of the EU directive 2010/63/EU governing the care and use of experimental animals, and following local laws and regulations [Finnish Act on the Protection of Animals Used for Scientific or Educational Purposes (497/2013), Government Decree on the Protection of Animals Used for Scientific or Educational Purposes (564/2013)]. The use of animals for collecting tissues was reviewed and approved by Laboratory Animal Center, Helsinki Institute of Life Sciences, University of Helsinki (internal license KEK17-012).

## Statistics

For statistical analysis, non-normalized raw data was used, with the exceptions of kinase assay for which total ERK1/2-normalized values, qPCR for which  $\Delta$ Ct values, and western blotting for which  $\beta$ -actin-adjusted values were used. Statistical analyses were performed using IBM SPSS Statistics 25 software. Statistical significance was evaluated with randomized block ANOVA (experiment and treatment as factors) followed by Dunnett's post hoc test. Differences at the level of  $P < 0.05$  were considered statistically significant.

## Results

### The effect of PKC agonists and inhibitors on cardiac fibroblast viability

We first examined the effect of PKC agonists and inhibitors on the viability of CFs. Based on the MTT assay, 24-h exposure to PMA at the concentrations of 10 nM and 100 nM caused small 23% (95% CI 11–34;  $P=0.004$ ) and 14% (95% CI 0–30;  $P=0.062$ ) decreases, respectively, in viability of CFs (Supplemental Fig. S1). Exposure to partial PKC agonist HMI-1b11 at the concentration of 30  $\mu$ M decreased metabolic activity 70% (95% CI 54–85;  $P<0.001$ ) but at 10  $\mu$ M concentration HMI-1b11 slightly increased it (28%; 95% CI 5–52;  $P=0.025$ ), compared to control. A treatment with the pan-PKC inhibitor Gö6983 had no effect on CF viability, while the inhibitor of classical PKCs (Gö6976) decreased cell viability concentration-dependently; 17% (95% CI 12–22) at 1  $\mu$ M concentration and 39% (95% CI 30–48;  $P=0.004$ ) at 10  $\mu$ M concentration. Based on the LDH assay results, only HMI-1b11 at the highest 30  $\mu$ M concentration exhibited a noticeable cytotoxic response; after a 24-h exposure the LDH release was 35% of the maximal (95% CI 27–45;  $P<0.001$ ; Supplemental Fig. S1). PMA and the PKC inhibitors induced less than 10% increase in cytotoxicity even with the highest concentrations. Concentrations for the proliferation and transdifferentiation experiments were selected based on the present results regarding toxicity and previous reports regarding *in vitro* efficacy of the compounds (Sarajärvi et al., 2018; Talman et al., 2013). Furthermore, as PMA induces down-regulation of several PKC isoforms at 100 nM (Johnson et al., 1995), the 10 nM concentration was chosen to avoid down-regulation.

### The effect of PKC agonists and inhibitors on ERK1/2 phosphorylation in cardiac fibroblasts

To confirm the effect of PMA and HMI-1b11 on PKC, activation of mitogen activated protein kinase kinase–extracellular signal-regulated kinase (MEK–ERK) pathway, a known downstream signaling pathway of PKC (Mackay and Twelves, 2007; Schönwasser et al.,

1998), was studied by measuring ERK1/2 phosphorylation in CFs using AlphaLISA® assay. A 30-min exposure to PMA at 10 nM concentration and HMI-1b11 at 10  $\mu$ M concentration induced 2.9-fold (95% CI 1.9–4.0;  $P=0.016$ ) and 2.6-fold (95% CI 1.8–3.5;  $P=0.037$ ) increases, respectively, in the amount of p-ERK1/2 compared to DMSO-control (Fig. 1A). Moreover, the increases in p-ERK1/2 were inhibited with the pan-PKC inhibitor Gö6983 but not with the cPKC inhibitor Gö6976, suggesting that PKC agonist-mediated ERK1/2 activation is mediated by nPKCs in CFs.

### **The effect of PKC agonists and inhibitors on PKC protein levels in cardiac fibroblasts**

We then analyzed PKC protein levels to verify the expression of selected isoenzymes in mouse CFs and to assess whether PMA or HMI-1b11 cause PKC down-regulation in our experimental design. Based on our previous RNA sequencing data (Talman et al., 2018a; Talman et al., 2018b), the main PKC isoforms expressed in mouse heart are  $\alpha$ ,  $\delta$ ,  $\epsilon$ ,  $\eta$ , and  $\lambda$  [the mouse homologue of human PKC $\lambda$  (Webb et al., 2000)] (Supplemental Fig. S2). As the C1 domain of atypical PKC $\lambda$  does not bind C1 domain ligands analogous to DAG, including PMA and HMI-1b11 (Steinberg, 2008; Talman et al., 2014b), only the classical ( $\alpha$ ) and novel ( $\delta$ ,  $\epsilon$ , and  $\eta$ ) isoforms of these five isoforms abundant in mouse hearts were selected for western blot analysis. Firstly, all four isoforms were detected in total cell homogenates and thus their expression in mouse cardiac (myo)fibroblasts was verified (Fig. 1B–F). Secondly, neither PMA at 10 nM concentration nor HMI-1b11 at 10  $\mu$ M concentration had effect on PKC $\alpha$ , PKC $\epsilon$  or PKC $\eta$  protein levels after 48-h exposure. However, both PKC activators induced a minor down-regulation of PKC $\delta$ , which was not inhibited by co-exposure to the pan-PKC inhibitor Gö6983. The PMA-induced decrease was 25% (95% CI 13–37;  $P=0.040$ ) and HMI-1b11-induced decrease 34% (95% CI 20–48;  $P=0.003$ ) compared to control.

### **The effect of PKC agonists and inhibitors on cardiac fibroblast phenotype**

To characterize the primary cell culture and to study the phenotype of CFs, we used discoidin domain receptor 2 (DDR2) as a marker of fibroblasts and  $\alpha$ -smooth muscle actin ( $\alpha$ -

SMA) as a marker of myofibroblasts. DDR2 was chosen because within the heart it is only expressed in fibroblasts (Goldsmith et al., 2004).  $\alpha$ -SMA, on the other hand, is expressed in smooth muscle cells, but also serves as a marker of activated and transdifferentiated fibroblasts, myofibroblasts, which have a key role in scar formation and myocardial remodeling after cardiac injury (van den Borne et al., 2010). Based on DDR2 expression, approximately 98% of the cells in the primary cultures were CFs (Supplemental Fig. S4). Moreover, when cultured in mere cell culture medium, CFs acquired a myofibroblast phenotype within 72 h from plating as demonstrated by  $\alpha$ -SMA expression. The relative  $\alpha$ -SMA staining intensity increased 5.8-fold (95% CI 1.9–9.7;  $P=0.030$ ) between 24 h and 72 h time points (Supplemental Fig. S4). This spontaneous phenotypic change (previously reported in Wang et al., 2003) was then further utilized to investigate the effects of PKC agonists on CF transdifferentiation. Both PKC agonists, PMA at 10 nM and HMI-1b11 at 10  $\mu$ M concentration, inhibited fibroblast transdifferentiation to myofibroblasts after 48-h exposure (Fig. 2A–B). PMA induced a 56% reduction (95% CI 47–65;  $P=0.011$ ) in the integrated intensity of  $\alpha$ -SMA staining compared to DMSO-control (Fig. 2C). This decrease appeared to be cPKC-dependent as it was prevented with both the cPKC inhibitor Gö6976 and the pan-PKC inhibitor Gö6983. Also HMI-1b11 decreased the expression of  $\alpha$ -SMA by 34% (95% CI 33–35;  $P=0.018$ ), and the inhibitors partially attenuated the effect. The inhibitors alone had no effect on  $\alpha$ -SMA expression (Fig. 2C).

### **The effect of PKC agonists and inhibitors on cardiac fibroblast proliferation**

To investigate the effect of PKC activation on cell cycle activity of CFs, HCA of BrdU and Ki67 stainings was utilized. After a 48-h exposure, PMA induced a 33% decrease (95% CI 24–42;  $P=0.018$ ) in BrdU-positive and a 36% decrease (95% CI 8–64;  $P=0.008$ ) in Ki67-positive CFs compared to DMSO-control (Fig. 3). These decreases were nPKC-dependent as they were inhibited with the pan-PKC inhibitor Gö6983 but not with the cPKC inhibitor Gö6976. PKC inhibitors alone had no effect on cell cycle activity of CF when compared to

DMSO. The partial PKC agonist HMI-1b11 had no effect on BrdU-positive cells but induced a 15% (95% CI 0–30) decrease in Ki67-positive cells.

### **The effect of PKC agonists and inhibitors on gene expression in cardiac fibroblasts**

To study the effects of PKC activation on the expression of genes related to cardiac fibrosis, we analyzed mRNA levels with qPCR after treating CFs with the PKC agonists and/or inhibitors for 48 h. Both PKC agonists decreased the expression of several genes that encode structural proteins of cardiac extracellular matrix (Fig. 4). PMA decreased the expression of type I and III collagen encoding genes *Col1a1* (47%; 95% CI 34–60;  $P=0.003$ ; Fig. 4A) and *Col3a1* (64%; 95% CI 59–69;  $P<0.001$ ; Fig. 4C), and tended to decrease *Col1a2* (26%; 95% CI 15–37; Fig. 4B) as well as glycoprotein fibronectin encoding *Fn1* gene (30%; 95% CI 17–43; Fig. 4D). Compound HMI-1b11 decreased the expression of *Col3a1* (53%; 95% CI 43–63;  $P=0.007$ ; Fig. 4C) and slightly *Fn1* (22%; 95% CI 15–29; Fig. 4D) compared to DMSO-control. All of these decreases were nPKC-dependent as they were inhibited or attenuated with the pan-PKC inhibitor Gö6983 but not with the cPKC inhibitor Gö6976. In fact, co-exposure to Gö6976 tended to further decrease the mRNA levels of these structural protein encoding genes, in particular with the weaker PKC activator HMI-1b11.

The expression of *Postn* gene that encodes for the matricellular protein periostin decreased after a 48-h exposure to PKC agonists (Fig. 4E): 60% in PMA-treated cells (95% CI 39–81;  $P=0.005$ ) and 48% in HMI-1b11-treated cells (95% CI 28–68;  $P=0.022$ ). The effect was inhibited with both inhibitors, suggesting it was cPKC-dependent. At the same time, the mRNA level of *Acta2* that encodes contractile protein  $\alpha$ -SMA was not affected by exposure to PMA but was 36% lower (95% CI 34–38;  $P=0.004$ ) in HMI-1b11-treated cells when compared to control (Fig. 4F). The cPKC inhibitor Gö6976 increased the transcription of *Acta2* with or without co-exposure to PKC agonists while the pan-PKC inhibitor Gö6983 had no effect on *Acta2* expression. Expression of TGF- $\beta$ 1 encoding gene *Tgfb1* was up-regulated

by HMI-1b11 (54%; 95% CI 34–74;  $P=0.019$ ), while co-exposure to the inhibitors, especially Gö6983, attenuated the effect (Fig. 4G). Gö6976 alone increased the expression of *Tcf21* (transcription factor 21 encoding) gene ( $P=0.011$ ; Fig. 4H) compared to DMSO. Similarly, co-exposure to PMA and Gö6983 increased *Tcf21* mRNA levels when compared to DMSO ( $P=0.023$ ). Gö6976, with or without co-exposure to the PKC agonists, tended to slightly increase the expression of *Myh10* (myosin heavy chain 10 encoding gene) as well (Fig. 4I).

Moreover, PKC agonists and inhibitors had distinct effects on the expression of *Mmp2* (Fig. 4J) and *Mmp9* (Fig. 4K) that encode matrix metalloproteinases. PMA or HMI-1b11 alone had no effect on the expression of *Mmp2* whereas co-exposure to the cPKC inhibitor Gö6976 increased the expression when compared to DMSO-control: PMA + Gö6976, 52% (95% CI 2–102;  $P=0.037$ ); and HMI-1b11 + Gö6976, 80% (95% CI 27–133;  $P=0.014$ ). On the other hand, the expression of *Mmp9* increased 2.6-fold (95% CI 1.6–3.7;  $P=0.035$ ) compared to control after a 48-h exposure to PMA. In HMI-1b11-treated cells the increase was more modest (1.3-fold; 95% CI 0.7–1.8). In both cases the effect was attenuated with co-exposure to Gö6976 and Gö6983, suggesting it was cPKC-dependent.

## Discussion

Although numerous studies have been published regarding the role of PKC in heart failure, the results are conflicting and sometimes difficult to interpret. Moreover, the roles of individual PKC isoforms in CF proliferation and transdifferentiation, two central processes in the development of fibrosis, and the potential of targeting PKC with pharmacological compounds to inhibit pathological fibrosis have not been fully elucidated. Therefore, in this study our aim was to characterize CF proliferation, phenotype, and gene expression in response to selected proprietary and commercially available PKC agonists and inhibitors.

Overall, previous reports suggest that PKC isoforms play a role in cardiac fibrosis and remodeling. Their partially overlapping and redundant roles as well as compensatory changes in the expression of other PKC isoforms in knockdown models however complicate the interpretation of the results and may explain the sometimes conflicting outcomes (Gallegos and Newton, 2008; Klein et al., 2005; Song et al., 2015). Furthermore, the effect of PKC activation or inhibition is often cell type and stimulus-dependent. In addition, the context-dependent regulation of PKC activity is not thoroughly understood. Using pharmacological tools for modulating PKC is not straightforward either as even compounds that were originally reported to be isoform selective have proved out to exert cellular actions also via other PKC isoforms and kinases (Steinberg and Sussman, 2005; Wu-Zhang and Newton, 2013). Additionally, not much is known about the role of PKC specifically in CFs. Most reports concerning the effects of PKC in cardiac fibrosis are from *in vivo* studies, which makes it difficult to decipher whether the effects on fibroblasts are direct or indirect. Better understanding of the role of PKC in CF activation would help the identification of the PKC isoforms that could serve as therapeutic targets for the treatment of adverse myocardial remodeling.



All PKC agonists and modulators used in this study proved to be relatively non-toxic to mouse CFs. Only compounds HMI-1b11 and Gö6976 with the highest concentrations tested (30  $\mu$ M and 10  $\mu$ M, respectively) showed substantial toxicity. Based on the HCA, PMA-induced activation of nPKCs decreased CF proliferation. Parallel decrease in the viability of PMA-treated cells as measured by the MTT assay, may also be explained with decreased cell division and thus lower cell density compared to control. Based on current knowledge, the activation and proliferation of resident fibroblasts represent the most important source of myofibroblasts in the fibrotic heart (Tallquist and Molkentin, 2017). Thus inhibiting both CF transdifferentiation and proliferation might have potential as therapeutic strategy for pathological fibrosis. In our study, both PKC agonists decreased  $\alpha$ -SMA expression, a hallmark of CF transdifferentiation, although PMA was more effective compared to partial agonist HMI-1b11. In addition to  $\alpha$ -SMA, periostin has been described as an underlying marker of cardiac myofibroblasts (Kanisicak et al., 2016). In our study, the changes observed in the expression of *Postn* in response to PKC activators and inhibitors were comparable to the changes noted in  $\alpha$ -SMA protein levels. Taken together, our results suggest that cPKCs are responsible for the PKC activator-induced inhibition of CF transdifferentiation. Moreover, the expression of collagen-encoding genes showed comparable nPKC-dependent as cell proliferation, indicating that PKC agonists may attenuate the production of new matrix proteins.

Interestingly, the changes seen in *Acta2* mRNA levels were not parallel to those in  $\alpha$ -SMA protein levels. This poor correlation between gene and protein expression could be due to timing: both analyses were done after 48-h compound exposures (72 h after cell isolation). Additionally, it is possible that PKC activation does not actually regulate  $\alpha$ -SMA expression on mRNA level but on later stages of the protein synthesis or degradation processes. Another interesting finding was the Gö6976-induced increase in *Acta2* mRNA levels, with or without co-exposure to PKC agonists. Considering Gö6976 has been shown to be a highly promiscuous inhibitor of other kinases besides classical PKC isoenzymes (Anastassiadis et

al., 2011; Davies et al., 2000), it can be speculated that this effect on *Acta2* expression is likely PKC-independent.

While several different markers used in the present study were regulated by PKC agonists and inhibitors, not all genes generally associated with fibrosis were affected or the effect was ambiguous. This in part demonstrates the complex nature of fibrosis and the numerous factors that take part in regulating fibrotic responses. Eventually, what takes place on tissue level, depends not only of the sum of all different factors, but also cooperation between different cell types. This can for example explain the unexpected increase in *Tgfb1* expression in CFs in response to PKC agonists. While TGF- $\beta$  induces myofibroblast transdifferentiation and enhances collagen production (Petrov et al., 2002), it is produced by several cell types *in vivo* and has multiple functions and roles in cardiac tissue during injury and remodeling (Dobaczewski et al., 2011).

Based on our previous RNA sequencing data (Talman et al., 2018a; Talman et al., 2018b), the main cPKCs and nPKCs expressed in adult mouse heart are  $\alpha$ ,  $\delta$ ,  $\epsilon$ , and  $\eta$ , which coincides with the analysis from Schreiber et al. (2001). Our present results indicate that the main cPKC isoform in mouse CFs is PKC $\alpha$ , moreover suggesting that PKC $\alpha$  regulates myofibroblast transdifferentiation. This is in line with the study by Gao et al. (2003), which showed that inhibition of PKC with calphostin C or deletion of PKC $\alpha$  with antisense PKC $\alpha$  oligodeoxynucleotides inhibited TGF $\beta$ -induced  $\alpha$ -SMA expression in rat aortic adventitial fibroblasts. Furthermore, we show that the main nPKCs expressed in the mouse heart are also expressed in CFs, thus suggesting that proliferation and collagen production in CFs are regulated via PKC $\delta$ , PKC $\epsilon$ , and/or PKC $\eta$ . On the other hand, long-term PKC activation by PMA causes down-regulation of PKC protein levels through proteasome-dependent and independent degradation (Young et al., 1987). Interestingly, 48-h exposures to PMA (at 10 nM) or HMI-1b11 (at 10  $\mu$ M) tended to down-regulate PKC $\delta$ , but not other isoenzymes. This minor down-regulation was comparable with that reported in SH-SY5Y neuroblastoma cells

after a 24-h exposure to 10  $\mu$ M HMI-1b11, but not as noticeable as in SH-SY5Y cells or cardiomyocytes treated with 100 nM PMA (Johnson et al., 1995; Sarajärvi et al., 2018). This together with our data demonstrating nPKC-mediated ERK1/2 activation in response to PMA or HMI-1b11 further supports the conclusion that the observed effects are due to PKC activation and not inhibition by downregulation.

It is noteworthy that the cells used were isolated from healthy adult female mice. PKC isoform expressions and thereby PKC-mediated signaling may change in diseased state, likely resulting in changes in the effects of PKC targeted compounds. Furthermore, it is possible that the age and the sex of the animals used could explain some of the discrepancies of the present results with previous studies. However, as most of the previous work has been conducted *in vivo* and using rats, we consider that the drastic difference of *in vivo* and *in vitro* conditions as well as the species differences are more plausible causes for the discrepancies observed. Another limitation of the present study are the pharmacological tools targeting multiple PKC isoenzymes but also other kinases. However, parallel usage of Gö6976 and Gö6983 provides a valuable tool to analyze whether an effect is a result of nPKC activity, cPKC activity, or PKC-independent. Furthermore, using the inhibitors in combination with C1 domain-targeting PKC activators, which only bind to two other serine-threonine kinases, protein kinase D and dystrophy kinase-related Cdc42 binding kinase (MRCK) (Colón-González and Kazanietz, 2006; Talman et al., 2014a), further strengthens the conclusion of PKC-mediated effects. Isoenzyme-specific silencing could be used to investigate the role of individual PKC isoforms in CFs. Redundant roles of closely related PKC isoforms and compensatory expression changes in other isoforms may, however, limit the conclusions from such experiments. Furthermore, PKC also has non-catalytic functions (Cameron et al., 2008; Ling et al., 2007; Zeidman et al., 1999), mainly via protein-protein-interactions, and thus genetic silencing and pharmacological tools targeting certain PKC isoforms may not always produce similar functional outcomes.

In conclusion, by characterizing mouse CFs in response to several different PKC agonists and inhibitors, we revealed that PKC agonists: (1) inhibit CF transdifferentiation into myofibroblasts, (2) decrease CF proliferation, and (3) decrease expression of collagen encoding genes in CFs. Moreover, we discovered that CF transdifferentiation is regulated via cPKCs, whereas CF proliferation and collagen gene expression are regulated via nPKCs. Overall, our results suggests that activation of PKC in CF may be a promising strategy to inhibit pathological cardiac remodeling. As down-regulation of PKC in response to irreversible PKC activation by ultrapotent PKC agonists such as PMA is considered to cause tumor-promotion previously attributed to PKC activation (Antal et al., 2015; Newton and Brognard, 2017), weaker or partial agonists that do not down-regulate PKC completely, such as the isophthalate HMI-1b11, represent promising leads for PKC-targeted antifibrotic therapies. Further studies in multicellular environment and pathophysiological context are however required to establish proof-of-concept.

## Acknowledgements

We thank Dr. Sini Kinnunen and Prof. Timo Myöhänen for sharing their expertise in the research methods, Dr. Harri Jääliñoja for providing support for the phenotypic analysis, and Ms. Annika Korvenpää for her technical assistance. Prof. Jari Yli-Kauhaluoma and Mr. Riccardo Provenzano (University of Helsinki) are kindly acknowledged for providing the compound HMI-1b11. The Light Microscopy Unit (Institute of Biotechnology and Helsinki Institute of Life Science, University of Helsinki) is acknowledged for providing instrumentation for the phenotypic analysis. The Biomedicum Imaging Unit (Helsinki Institute of Life Science, University of Helsinki) is acknowledged for providing instrumentation for the HCA.

## Author Contributions

*Participated in research design:* Karhu, Ruskoaho, and Talman

*Conducted experiments:* Karhu

*Performed data analysis:* Karhu and Talman

*Contributed to the writing of the manuscript:* Karhu, Ruskoaho, and Talman

## References

- Anastassiadis T, Deacon SW, Devarajan K, Ma H, Peterson JR (2011) Comprehensive assay of kinase catalytic activity reveals features of kinase inhibitor selectivity. *Nat Biotechnol* **29**: 1039-1045.
- Antal CE, Hudson AM, Kang E, Zanca C, Wirth C, Stephenson NL, Trotter EW, Gallegos LL, Miller CJ, Furnari FB, Hunter T, Brognard J, Newton AC (2015) Cancer-associated protein kinase C mutations reveal kinase's role as tumor suppressor. *Cell* **160**: 489-502.
- Boije af Gennäs G, Talman V, Yli-Kauhahuoma J, Tuominen RK, Ekokoski E (2011) Current status and future prospects of C1 domain ligands as drug targets. *Curr Top Med Chem* **11**: 1370-1392.
- Boije af Gennäs G, Talman V, Aitio O, Ekokoski E, Finel M, Tuominen RK, Yli-Kauhahuoma J (2009) Design, synthesis, and biological activity of isophthalic acid derivatives targeted to the C1 domain of protein kinase C. *J Med Chem* **52**: 3969-3981.
- Bowling N, Walsh RA, Song G, Estridge T, Sandusky GE, Fouts RL, Mintze K, Pickard T, Roden R, Bristow MR, Sabbah HN, Mizrahi JL, Gromo G, King GL, Vlahos CJ (1999) Increased protein kinase C activity and expression of Ca<sup>2+</sup>-sensitive isoforms in the failing human heart. *Circulation* **99**: 384-391.
- Boyle AJ, Kelly DJ, Zhang Y, Cox AJ, Gow RM, Way K, Itescu S, Krum H, Gilbert RE (2005) Inhibition of protein kinase C reduces left ventricular fibrosis and dysfunction following myocardial infarction. *J Mol Cell Cardiol* **39**: 213-221.
- Braun MU, Mochly-Rosen D (2003) Opposing effects of  $\delta$ - and  $\zeta$ -protein kinase C isozymes on cardiac fibroblast proliferation: use of isozyme-selective inhibitors. *J Mol Cell Cardiol* **35**: 895-903.
- Cameron AJ, Procyk KJ, Leitges M, Parker PJ (2008) PKC alpha protein but not kinase activity is critical for glioma cell proliferation and survival. *Int J Cancer* **123**: 769-779.

- Cohn JN, Ferrari R, Sharpe N (2000) Cardiac remodeling--concepts and clinical implications: a consensus paper from an international forum on cardiac remodeling. Behalf of an International Forum on Cardiac Remodeling. *J Am Coll Cardiol* **35**: 569-582.
- Colón-González F, Kazanietz MG (2006) C1 domains exposed: from diacylglycerol binding to protein-protein interactions. *Biochim Biophys Acta* **1761**: 827-837.
- Connelly KA, Kelly DJ, Zhang Y, Prior DL, Advani A, Cox AJ, Thai K, Krum H, Gilbert RE (2009) Inhibition of protein kinase C- $\beta$  by ruboxistaurin preserves cardiac function and reduces extracellular matrix production in diabetic cardiomyopathy. *Circ Heart Fail* **2**: 129-137.
- Davies SP, Reddy H, Caivano M, Cohen P (2000) Specificity and mechanism of action of some commonly used protein kinase inhibitors. *Biochem J* **351**: 95-105.
- Dobaczewski M, Chen W, Frangogiannis NG (2011) Transforming growth factor (TGF)- $\beta$  signaling in cardiac remodeling. *J Mol Cell Cardiol* **51**: 600-606.
- Ferreira JC, Koyanagi T, Palaniyandi SS, Fajardo G, Churchill EN, Budas G, Disatnik MH, Bernstein D, Brum PC, Mochly-Rosen D (2011) Pharmacological inhibition of  $\beta$ IIIPKC is cardioprotective in late-stage hypertrophy. *J Mol Cell Cardiol* **51**: 980-987.
- Gallegos LL, Newton AC (2008) Spatiotemporal dynamics of lipid signaling: protein kinase C as a paradigm. *IUBMB Life* **60**: 782-789.
- Gao PJ, Li Y, Sun AJ, Liu JJ, Ji KD, Zhang YZ, Sun WL, Marche P, Zhu DL (2003) Differentiation of vascular myofibroblasts induced by transforming growth factor- $\beta$ 1 requires the involvement of protein kinase C $\alpha$ . *J Mol Cell Cardiol* **35**: 1105-1112.
- Goldsmith EC, Hoffman A, Morales MO, Potts JD, Price RL, McFadden A, Rice M, Borg TK (2004) Organization of fibroblasts in the heart. *Dev Dyn* **230**: 787-794.
- Gulati A, Jabbour A, Ismail TF, Guha K, Khwaja J, Raza S, Morarji K, Brown TD, Ismail NA, Dweck MR, Di Pietro E, Roughton M, Wage R, Daryani Y, O'Hanlon R, Sheppard MN, Alpendurada F, Lyon AR, Cook SA, Cowie MR, Assomull RG, Pennell DJ, Prasad SK



- (2013) Association of fibrosis with mortality and sudden cardiac death in patients with nonischemic dilated cardiomyopathy. *JAMA* **309**: 896-908.
- Inagaki K, Koyanagi T, Berry NC, Sun L, Mochly-Rosen D (2008) Pharmacological inhibition of  $\epsilon$ -protein kinase C attenuates cardiac fibrosis and dysfunction in hypertension-induced heart failure. *Hypertension* **51**: 1565-1569.
- Johnson JA, Adak S, Mochly-Rosen D (1995) Prolonged phorbol ester treatment down-regulates protein kinase C isozymes and increases contraction rate in neonatal cardiac myocytes. *Life Sci* **57**: 1027-1038.
- Kanisicak O, Khalil H, Ivey MJ, Karch J, Maliken BD, Correll RN, Brody MJ, J Lin SC, Aronow BJ, Tallquist MD, Molkentin JD (2016) Genetic lineage tracing defines myofibroblast origin and function in the injured heart. *Nat Commun* **7**: 12260.
- Karhu ST, Välimäki MJ, Jumppanen M, Kinnunen SM, Pohjolainen L, Leigh RS, Auno S, Földes G, Boije Af Gennäs G, Yli-Kauhaluoma J, Ruskoaho H, Talman V (2018) Stem cells are the most sensitive screening tool to identify toxicity of GATA4-targeted novel small-molecule compounds. *Arch Toxicol* **92**: 2897-2911.
- Klein G, Schaefer A, Hilfiker-Kleiner D, Oppermann D, Shukla P, Quint A, Podewski E, Hilfiker A, Schroder F, Leitges M, Drexler H (2005) Increased collagen deposition and diastolic dysfunction but preserved myocardial hypertrophy after pressure overload in mice lacking PKC $\epsilon$ . *Circ Res* **96**: 748-755.
- Kong P, Christia P, Frangogiannis NG (2014) The pathogenesis of cardiac fibrosis. *Cell Mol Life Sci* **71**: 549-574.
- Ling M, Sunesson L, Larsson C (2007) Comparison of the PKC $\alpha$  and the PKC $\epsilon$  C1b domains: identification of residues critical for PKC $\epsilon$ -mediated neurite induction. *J Mol Biol* **368**: 951-965.
- Liu Q, Chen X, Macdonnell SM, Kranias EG, Lorenz JN, Leitges M, Houser SR, Molkentin JD (2009) Protein kinase C $\alpha$ , but not PKC $\beta$  or PKC $\gamma$ , regulates contractility and heart failure

- susceptibility: implications for ruboxistaurin as a novel therapeutic approach. *Circ Res* **105**: 194-200.
- Mackay HJ, Twelves CJ (2007) Targeting the protein kinase C family: are we there yet? *Nat Rev Cancer* **7**: 554-562.
- Mochly-Rosen D, Das K, Grimes KV (2012) Protein kinase C, an elusive therapeutic target? *Nat Rev Drug Discov* **11**: 937-957.
- Newton AC, Brognard J (2017) Reversing the paradigm: protein kinase C as a tumor suppressor. *Trends Pharmacol Sci* **38**: 438-447.
- Palaniyandi SS, Sun L, Ferreira JC, Mochly-Rosen D (2009) Protein kinase C in heart failure: a therapeutic target? *Cardiovasc Res* **82**: 229-239.
- Petrov VV, Fagard RH, Lijnen PJ (2002) Stimulation of collagen production by transforming growth factor- $\beta$ 1 during differentiation of cardiac fibroblasts to myofibroblasts. *Hypertension* **39**: 258-263.
- Sarajärvi T, Jäntti M, Paldanius KMA, Natunen T, Wu JC, Mäkinen P, Tarvainen I, Tuominen RK, Talman V, Hiltunen M (2018) Protein kinase C -activating isophthalate derivatives mitigate Alzheimer's disease-related cellular alterations. *Neuropharmacology* **141**: 76-88.
- Schreiber KL, Paquet L, Allen BG, Rindt H (2001) Protein kinase C isoform expression and activity in the mouse heart. *Am J Physiol Heart Circ Physiol* **281**: H2062-H2071.
- Schönwasser DC, Marais RM, Marshall CJ, Parker PJ (1998) Activation of the mitogen-activated protein kinase/extracellular signal-regulated kinase pathway by conventional, novel, and atypical protein kinase C isotypes. *Mol Cell Biol* **18**: 790-798.
- Shin HG, Barnett JV, Chang P, Reddy S, Drinkwater DC, Pierson RN, Wiley RG, Murray KT (2000) Molecular heterogeneity of protein kinase C expression in human ventricle. *Cardiovasc Res* **48**: 285-299.
- Shinde AV, Frangogiannis NG (2014) Fibroblasts in myocardial infarction: a role in inflammation and repair. *J Mol Cell Cardiol* **70**: 74-82.

- Simonis G, Briem SK, Schoen SP, Bock M, Marquetant R, Strasser RH (2007) Protein kinase C in the human heart: differential regulation of the isoforms in aortic stenosis or dilated cardiomyopathy. *Mol Cell Biochem* **305**: 103-111.
- Song M, Matkovich SJ, Zhang Y, Hammer DJ, Dorn GW, 2nd (2015) Combined cardiomyocyte PKC $\delta$  and PKC $\epsilon$  gene deletion uncovers their central role in restraining developmental and reactive heart growth. *Sci Signal* **8**: ra39.
- Steinberg SF (2012) Cardiac actions of protein kinase C isoforms. *Physiology (Bethesda)* **27**: 130-139.
- Steinberg SF (2008) Structural basis of protein kinase C isoform function. *Physiol Rev* **88**: 1341-1378.
- Steinberg SF, Sussman MA (2005) Cardiac hypertrophy served with protein kinase C $\epsilon$ :  $\delta$  isoform substitution available at additional cost. *Circ Res* **96**: 711-713.
- Tallquist MD, Molkentin JD (2017) Redefining the identity of cardiac fibroblasts. *Nat Rev Cardiol* **14**: 484-491.
- Talman V, Teppo J, Pöhö P, Movahedi P, Vaikkinen A, Karhu ST, Trost K, Suvitaival T, Heikkonen J, Pahikkala T, Kotiaho T, Kostiaisen R, Varjosalo M, Ruskoaho H (2018a) Molecular atlas of postnatal mouse heart development. *J Am Heart Assoc* **7**: e010378.
- Talman V, Teppo J, Pöhö P, Movahedi P, Vaikkinen A, Karhu ST, Trost K, Suvitaival T, Heikkonen J, Pahikkala T, Kotiaho T, Kostiaisen R, Varjosalo M, Ruskoaho H (2018b) RNA expression in postnatal mouse ventricular tissue. *GEO Gene Expression Omnibus*. <http://www.ncbi.nlm.nih.gov/geo/>, Accession no. GSE119530.
- Talman V, Ruskoaho H (2016) Cardiac fibrosis in myocardial infarction-from repair and remodeling to regeneration. *Cell Tissue Res* **365**: 563-581.
- Talman V, Gateva G, Ahti M, Ekokoski E, Lappalainen P, Tuominen RK (2014a) Evidence for a role of MRCK in mediating HeLa cell elongation induced by the C1 domain ligand HMI-1a3. *Eur J Pharm Sci* **55**: 46-57.
- Talman V, Provenzani R, Boije af Gennäs G, Tuominen RK, Yli-Kauhaluoma J (2014b) C1 domain-targeted isophthalates as protein kinase C modulators: structure-based design,

- structure-activity relationships and biological activities. *Biochem Soc Trans* **42**: 1543-1549.
- Talman V, Amadio M, Osera C, Sorvari S, Boije Af Gennäs G, Yli-Kauhahuoma J, Rossi D, Govoni S, Collina S, Ekokoski E, Tuominen RK, Pascale A (2013) The C1 domain-targeted isophthalate derivative HMI-1b11 promotes neurite outgrowth and GAP-43 expression through PKC $\alpha$  activation in SH-SY5Y cells. *Pharmacol Res* **73**: 44-54.
- Talman V, Tuominen RK, Boije af Gennäs G, Yli-Kauhahuoma J, Ekokoski E (2011) C1 Domain-targeted isophthalate derivatives induce cell elongation and cell cycle arrest in HeLa cells. *PLoS One* **6**: e20053.
- van den Borne SW, Diez J, Blankesteyn WM, Verjans J, Hofstra L, Narula J (2010) Myocardial remodeling after infarction: the role of myofibroblasts. *Nat Rev Cardiol* **7**: 30-37.
- Wang J, Chen H, Seth A, McCulloch CA (2003) Mechanical force regulation of myofibroblast differentiation in cardiac fibroblasts. *Am J Physiol Heart Circ Physiol* **285**: H1871-H1881.
- Webb BL, Hirst SJ, Giembycz MA (2000) Protein kinase C isoenzymes: a review of their structure, regulation and role in regulating airways smooth muscle tone and mitogenesis. *Br J Pharmacol* **130**: 1433-1452.
- Wu-Zhang AX, Newton AC (2013) Protein kinase C pharmacology: refining the toolbox. *Biochem J* **452**: 195-209.
- Young S, Parker PJ, Ullrich A, Stabel S (1987) Down-regulation of protein kinase C is due to an increased rate of degradation. *Biochem J* **244**: 775-779.
- Zeidman R, Lofgren B, Pahlman S, Larsson C (1999) PKC $\epsilon$ , via its regulatory domain and independently of its catalytic domain, induces neurite-like processes in neuroblastoma cells. *J Cell Biol* **145**: 713-726.

## Footnotes

The research was supported by the Finnish Foundation for Cardiovascular Research; Business Finland [project no. 40395/13, 3iRegeneration]; the Sigrid Jusélius Foundation; the Academy of Finland [grant 321564]; and the Finnish Cultural Foundation.

## Figure Legends

**Figure 1. The effect of PKC agonists and inhibitors on ERK1/2 phosphorylation and PKC protein levels in primary cardiac fibroblasts isolated from adult mice. (A)** For cellular kinase assay, the cells were exposed to PKC agonists (10 nM PMA or 10  $\mu$ M HMI-1b11) with or without PKC inhibitors (1  $\mu$ M Gö6976, 1  $\mu$ M Gö6983) 24 h after plating for 30 min. The amount of total ERK1/2 and phospho-ERK1/2 (p-ERK1/2) were quantified from cellular lysates using Alpha technology. The results are shown as ratio of p-ERK1/2 to total ERK1/2. **(B–F)** For western blotting, the cells were exposed to PKC agonists (10 nM PMA or 10  $\mu$ M HMI-1b11) with or without PKC inhibitor (1  $\mu$ M Gö6983) 24 h after plating for 48 h, lysed, and total proteins were extracted. **(B)** Representative western blots of PKC isoforms and respective  $\beta$ -actin blots as loading controls. The full blots are shown in Supplemental Fig. S3. **(C–F)** Relative densities of PKC isoform immunoreactive bands adjusted to the corresponding  $\beta$ -actin bands. **(C)** PKC $\alpha$ ; **(D)** PKC $\delta$ ; **(E)** PKC $\epsilon$ ; **(F)** PKC $\eta$ . Results are displayed as scatter plots showing data values from independent experiments (n=3), with mean indicated by a line and error bars representing standard deviation. The data are normalized to DMSO-control. \*\*P<0.01 vs. DMSO-control; \*P<0.05 vs. DMSO-control (randomized block ANOVA followed by Dunnett's post hoc test)

**Figure 2. The effect of PKC agonists and inhibitors on  $\alpha$ -smooth muscle actin ( $\alpha$ -SMA) expression in primary cardiac fibroblasts isolated from adult mice.** The cells were exposed to PKC agonists (10 nM PMA or 10  $\mu$ M HMI-1b11) with or without PKC inhibitors (1  $\mu$ M Gö6976, 1  $\mu$ M Gö6983) 24 h after plating for 48 h. At 72 h after plating the cells were fixed and stained. **(A–B)** Representative images of  $\alpha$ -SMA staining (original magnification 20 $\times$ ). **(C)** Quantified intensity of  $\alpha$ -SMA staining. Results are displayed as scatter plots showing data values from independent experiments (n=3), with mean indicated by a line and

error bars representing standard deviation. The data are normalized to DMSO-control.

\*P<0.05 vs. DMSO-control (randomized block ANOVA followed by Dunnett's post hoc test)

**Figure 3. The effect of PKC agonists and inhibitors on cell cycle activity of primary cardiac fibroblasts isolated from adult mice.** The cells were exposed to PKC agonists (10 nM PMA or 10  $\mu$ M HMI-1b11) with or without PKC inhibitors (1  $\mu$ M Gö6976, 1  $\mu$ M Gö6983) 24 h after plating for 48 h. At 72 h after plating the cells were fixed and stained. Representative images of **(A)** BrdU and **(B)** Ki67 staining (original magnification 10 $\times$ ). Quantifications for the proportion of **(C)** BrdU-positive cells and **(D)** Ki67-positive cells. Results are expressed as mean + standard deviation (n=3). \*\*P<0.01 vs. DMSO-control; \*P<0.05 vs. DMSO-control (randomized block ANOVA followed by Dunnett's post hoc test)

**Figure 4. The effect of PKC agonists and inhibitors on gene expression in primary cardiac fibroblasts isolated from adult mice.** The cells were exposed to PKC agonists (10 nM PMA or 10  $\mu$ M HMI-1b11) with or without PKC inhibitors (1  $\mu$ M Gö6976, 1  $\mu$ M Gö6983) 24 h after plating for 48 h. At 72 h after plating mRNA was extracted and measured by qPCR. The levels of transcripts were adjusted to the average of two housekeeping genes (18S and *Actb*) from the same samples. **(A)** *Col1a1*; **(B)** *Col1a2*; **(C)** *Col3a1*; **(D)** *Fn1*; **(E)** *Postn*; **(F)** *Acta2*; **(G)** *Tgfb1*; **(H)** *Tcf21*; **(I)** *Myh10*; **(J)** *Mmp2*; **(K)** *Mmp9*. Results are displayed as scatter plots showing data values from independent experiments (n=3), with mean indicated by a line and error bars representing standard deviation. The data are normalized to DMSO-control. \*\*\*P<0.001 vs. DMSO-control; \*\*P<0.01 vs. DMSO-control; \*P<0.05 vs. DMSO-control (randomized block ANOVA followed by Dunnett's post hoc test)

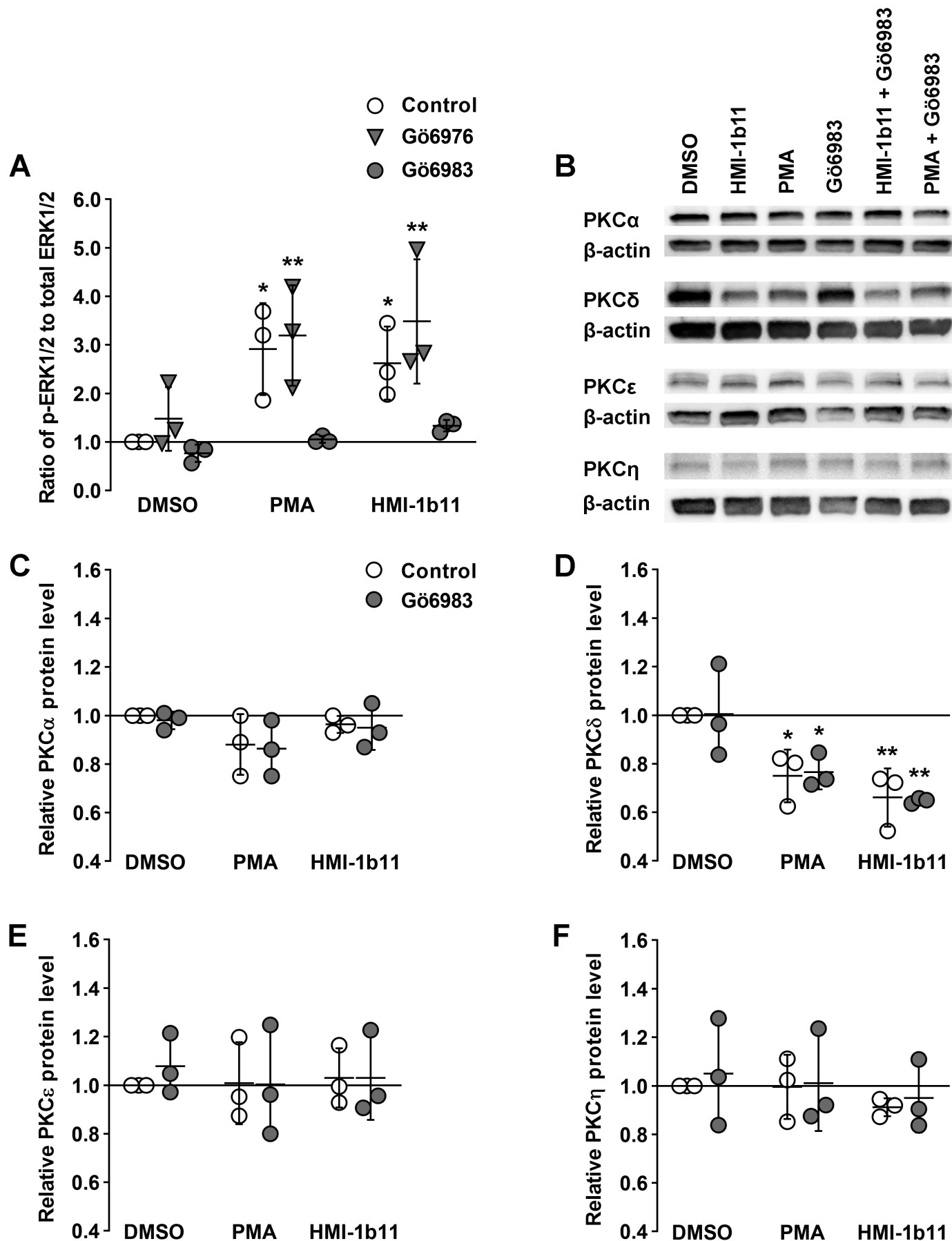
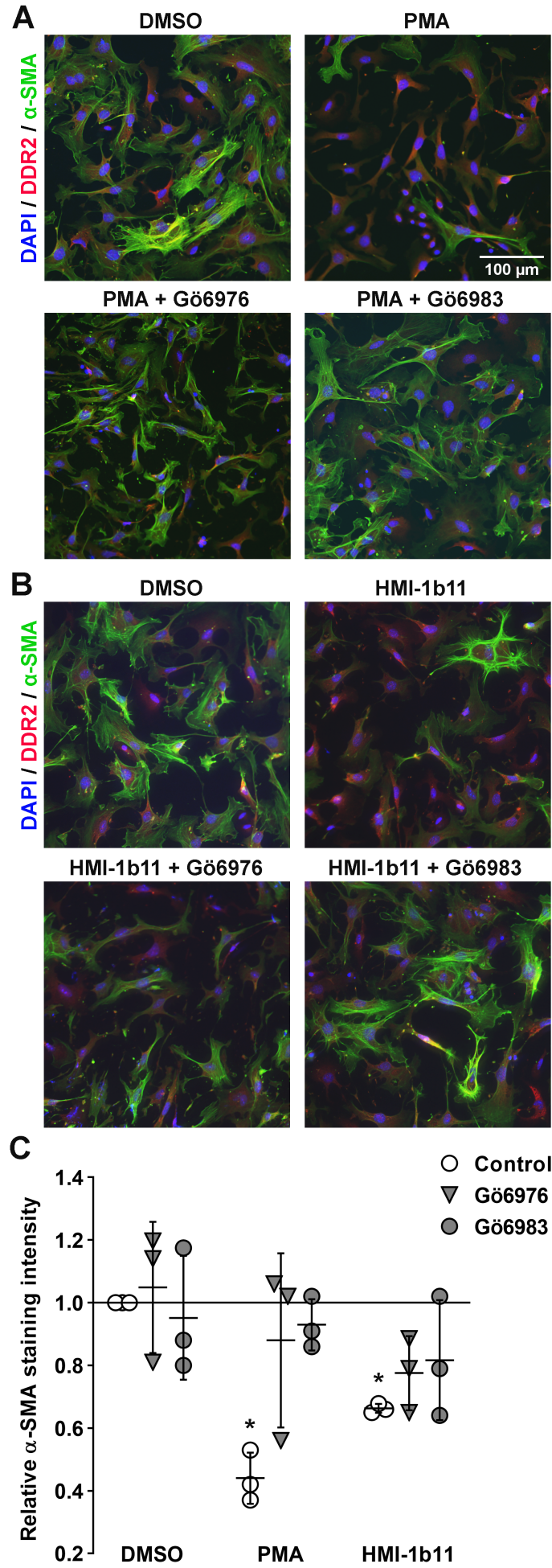


Figure 1





**Figure 2**

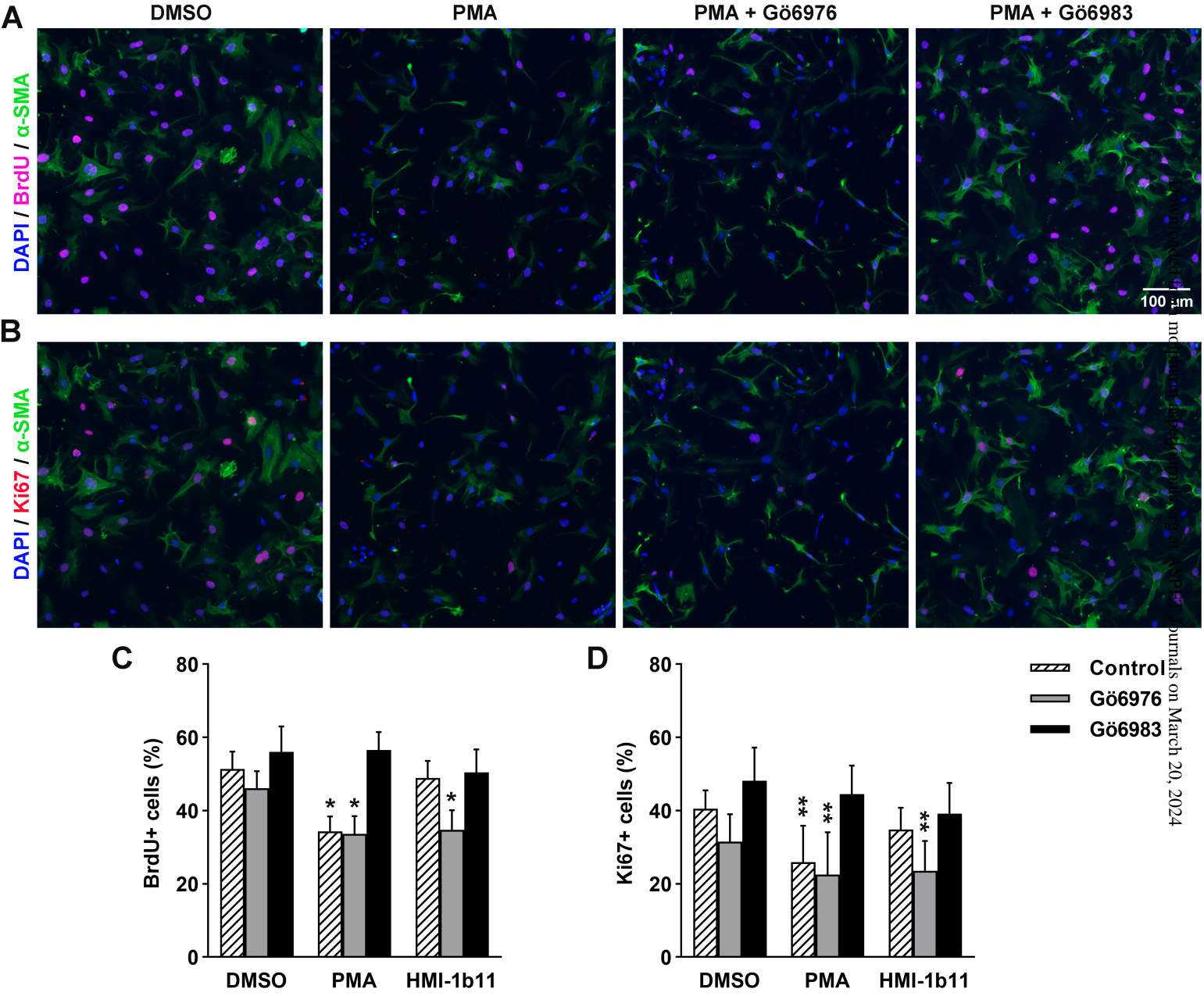
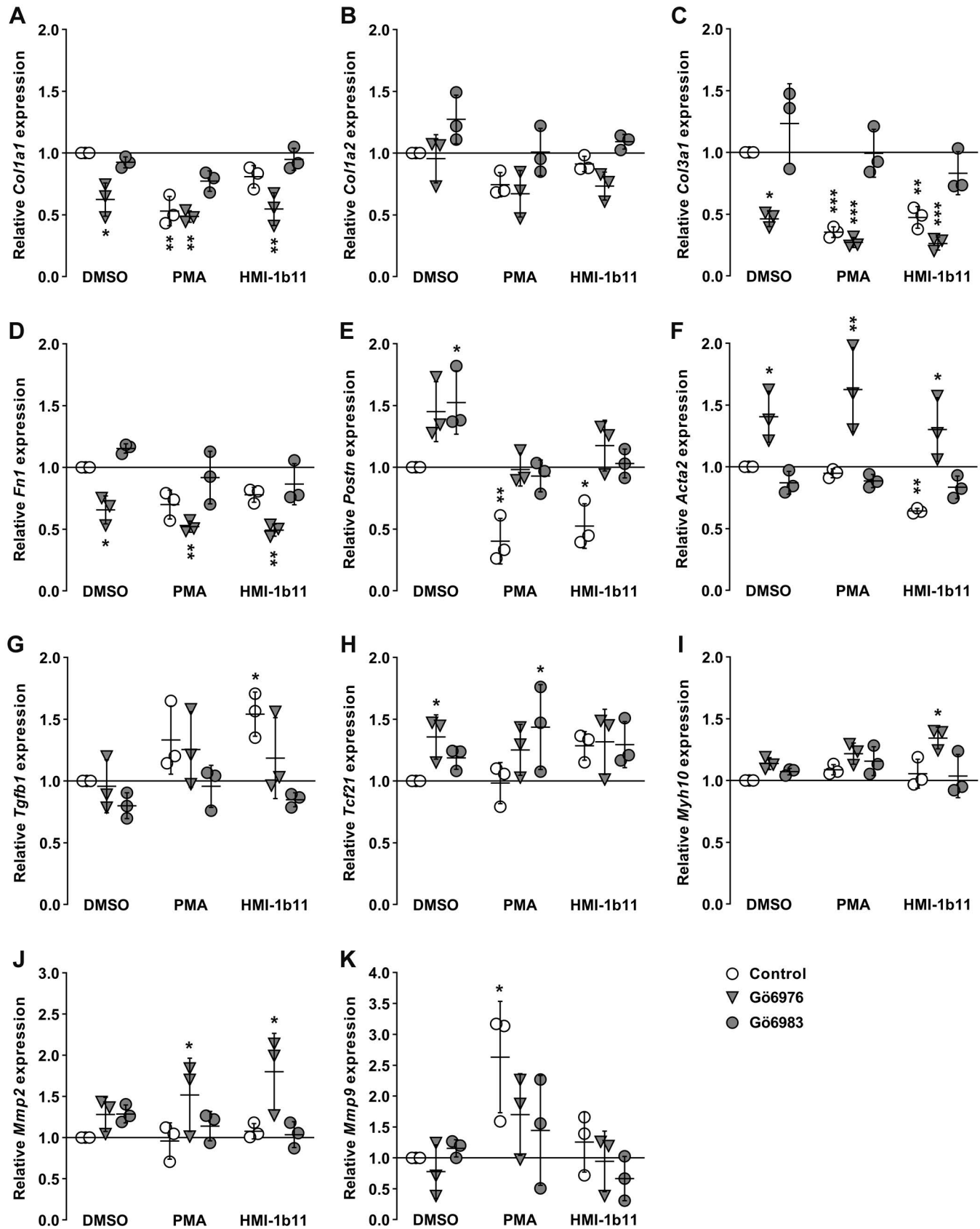


Figure 3



**Figure 4**

Molecular Pharmacology

MOLPHARM-AR-2020-000094

**Distinct regulation of cardiac fibroblast proliferation and transdifferentiation by classical and novel protein kinase C isoforms: possible implications for new antifibrotic therapies**

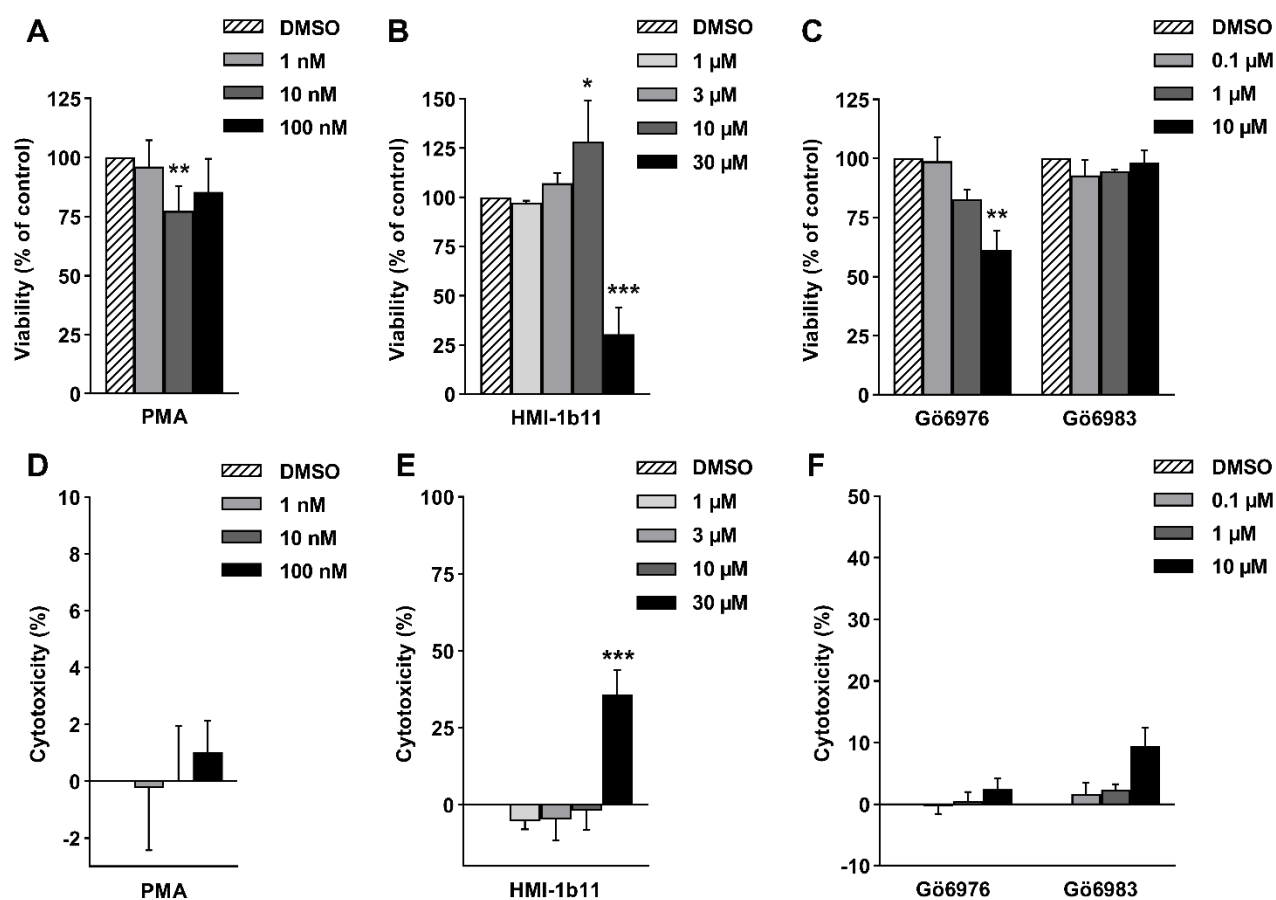
S. Tuuli Karhu, Heikki Ruskoaho, Virpi Talman\*

*Affiliations*

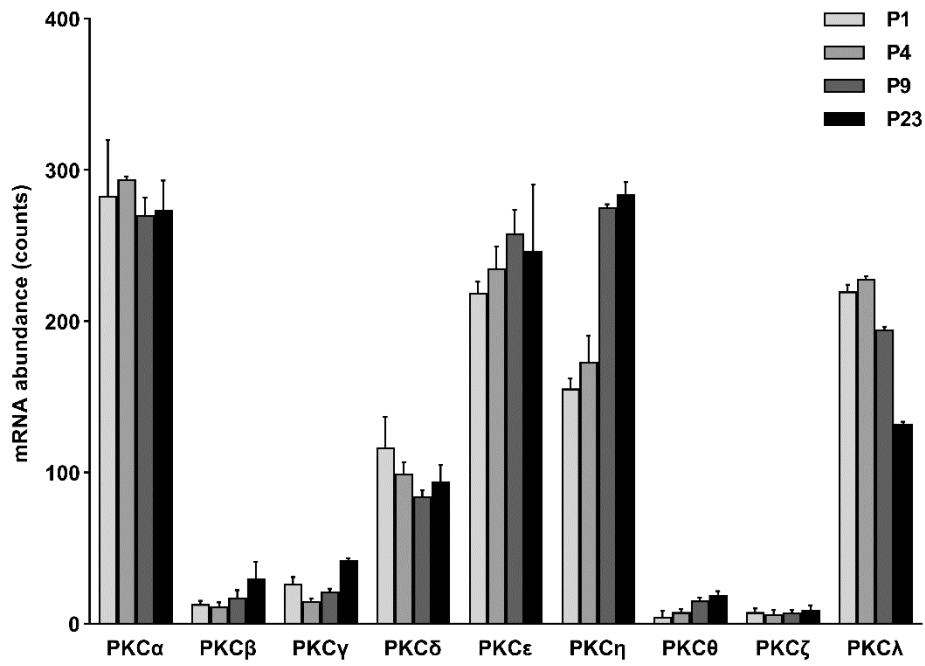
*STK, HR, and VT: Drug Research Program and Division of Pharmacology and Pharmacotherapy,  
Faculty of Pharmacy, University of Helsinki, Finland*

*\*Corresponding author*

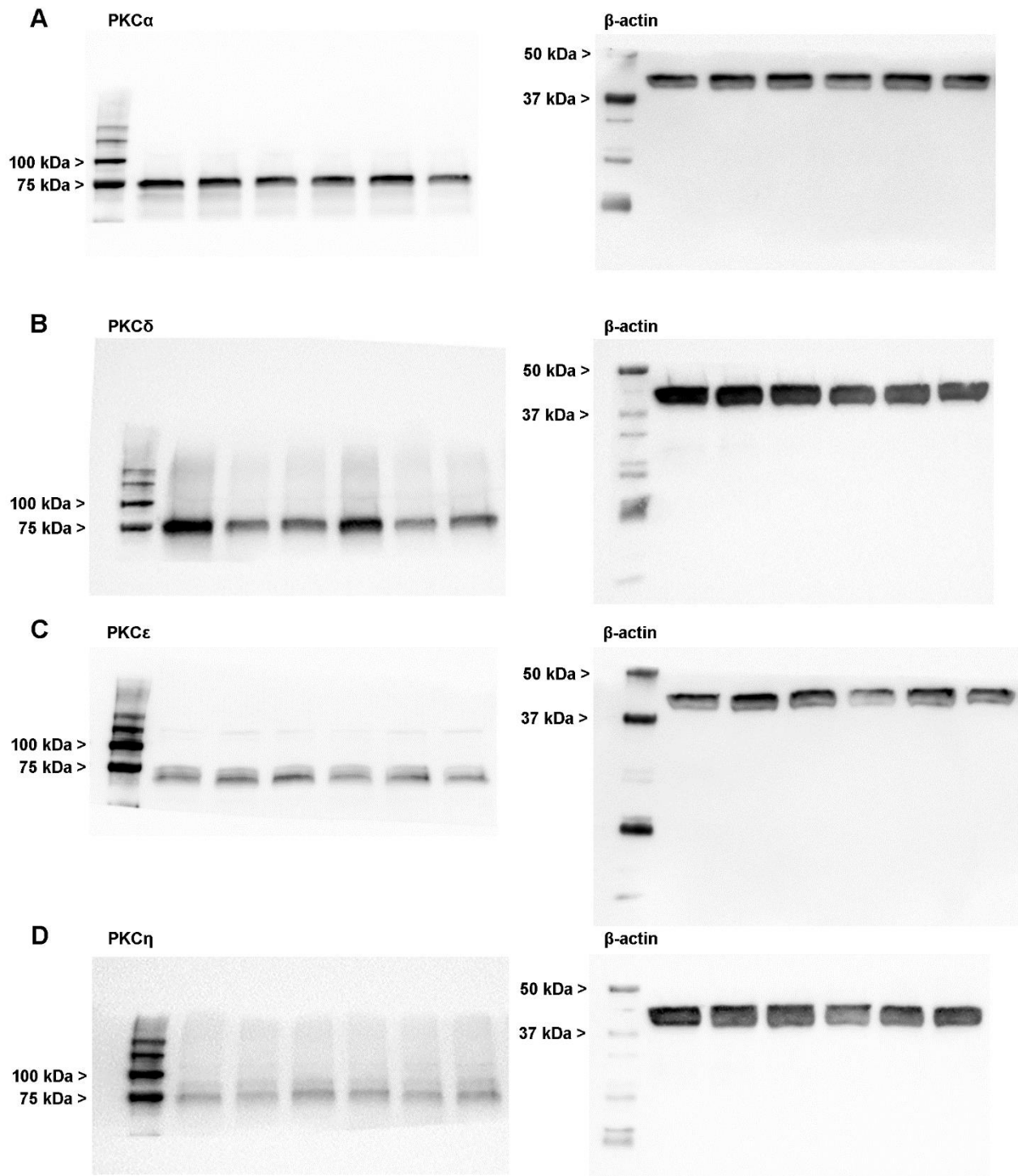
## Supplemental Data



**Supplemental Figure S1** The effect of PKC agonists and inhibitors on cell viability in primary cardiac fibroblasts isolated from adult mice. The cells were exposed to test compounds 24 h after plating for 24 h. At 48 h after plating the (A–C) MTT and (D–F) LDH assays were performed. Results are expressed as mean + standard deviation ( $n=3$ ). \*\*\* $P<0.001$  vs. DMSO; \*\* $P<0.01$  vs. DMSO; \* $P<0.05$  vs. DMSO (randomized block ANOVA followed by Dunnett's post hoc test)

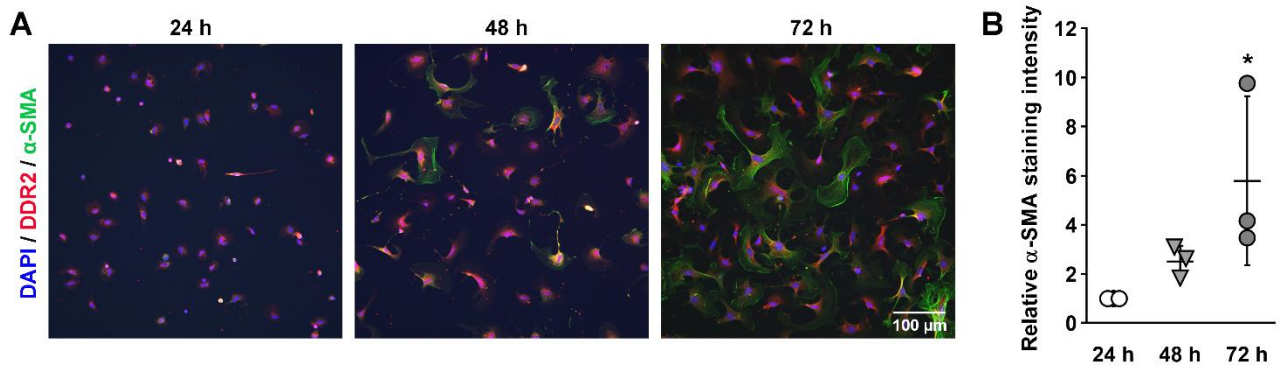


**Supplemental Figure S2** PKC isoform mRNA expression in neonatal mouse ventricles at postnatal days (P) 1, 4, 9, and 23. Results are expressed as mean + standard deviation (n=3). The data is from Talman et al., 2018a; Talman et al., 2018b



**Supplemental Figure S3** The original western blot images of PKC isoform (left panel) and corresponding loading control (right panel) immunoreactive bands presented in Figure 1B





**Supplemental Figure S4** Cardiac fibroblast phenotype in culture 24–72 h after isolation. Cardiac fibroblasts isolated from adult mice were cultured for 24–72 h after which they were fixed and stained. **(A)** Representative images of fibroblast culture at 24 h, 48 h, and 72 h after isolation (original magnification 20 $\times$ ). **(B)** Quantified intensity of  $\alpha$ -smooth muscle actin ( $\alpha$ -SMA) staining. Results are displayed as scatter plots showing data values from independent experiments ( $n=3$ ), with mean indicated by a line and error bars representing standard deviation. The data are normalized to 24 h. \* $P<0.05$  vs. 24 h (randomized block ANOVA followed by Dunnett's post hoc test)



## **References**

Talman V, Teppo J, Pöhö P, Movahedi P, Vaikkinen A, Karhu ST, Trost K, Suvitaival T, Heikkonen J, Pahikkala T, Kotiaho T, Kostiaainen R, Varjosalo M, Ruskoaho H (2018a) Molecular atlas of postnatal mouse heart development. *J Am Heart Assoc* **7**: e010378.

Talman V, Teppo J, Pöhö P, Movahedi P, Vaikkinen A, Karhu ST, Trost K, Suvitaival T, Heikkonen J, Pahikkala T, Kotiaho T, Kostiaainen R, Varjosalo M, Ruskoaho H (2018b) RNA expression in postnatal mouse ventricular tissue. *GEO Gene Expression Omnibus*. <http://www.ncbi.nlm.nih.gov/geo/>, Accession no. GSE119530.